*International Journal of Minerals, Metallurgy and Materials*
*Volume 22, Number 11, November 2015, Page 1199*
**DOI: 10.1007/s12613-015-1185-9**

# Microstructure and properties of Cu–Ti–Ni alloys

*Jia Liu*[1)], *Xian-hui Wang*[1,2)], *Ting-ting Guo*[2)], *Jun-tao Zou*[1)], *and Xiao-hong Yang*[1)]

1) Shaanxi Key Laboratory of Electrical Materials and Infiltration Technology, School of Materials Science and Engineering, Xi'an University of Technology, Xi'an 710048, China

2) Institute for Frontier Materials, Waurn Ponds, Deakin University, Victoria 3220, Australia

(Received: 6 February 2015; revised: 27 August 2015; accepted: 10 September 2015)

**Abstract:** The effects of Ni addition and aging treatments on the microstructure and properties of a Cu–3Ti alloy were investigated. The microstructure and precipitation phases were characterized by X-ray diffraction, scanning electron microscopy, and transmission electron microscopy; the hardness, electrical conductivity, and elastic modulus of the resulting alloys were also tested. The results show that Ni addition increases the electrical conductivity and elastic modulus, but decreases the hardness of the aged Cu–3Ti alloy. Within the range of the experimentally investigated parameters, the optimal two-stage aging treatment for the Cu–3Ti–1Ni and Cu–3Ti–5Ni alloy was 300°C for 2 h and 450°C for 7 h. The hardness, electrical conductivity, and elastic modulus of the Cu–3Ti–1Ni alloy were HV 205, 18.2% IACS, and 146 GPa, respectively, whereas the hardness, electrical conductivity, and elastic modulus of the Cu–3Ti–5Ni alloy were HV 187, 31.32% IACS, and 147 GPa, respectively. Microstructural analyses revealed that β′-$Ni_3Ti$ and β′-$Cu_4Ti$ precipitate from the Cu matrix during aging of the Cu–3Ti–5Ni alloy and that some residual NiTi phase remains. The increased electrical conductivity is ascribed to the formation of NiTi, β′-$Ni_3Ti$, and β′-$Cu_4Ti$ phases.

**Keywords:** copper alloys; aging; microstructure; hardness; electrical conductivity; elastic modulus

## 1. Introduction

Because of their excellent electrical and thermal conductivity and good corrosion resistance, Cu alloys are widely used in various electrical connections [1–2]. Among these Cu alloys, Cu–Be alloy exhibits a good compromise between mechanical strength and electrical conductivity. However, the beryllium oxide generated during the process of manufacturing Cu–Be alloy poses environmental hazards. Consequently, the development of a suitable material to replace Cu–Be alloy is an important research topic. Because age-hardened Cu–Ti alloy exhibits good mechanical properties, it is regarded as the most suitable substitute for expensive and toxic Cu–Be alloy. Numerous investigations of the precipitation strengthening mechanism of Cu–Ti alloys have been reported in the literatures [3–8]. Nagarjuna *et al.* [9–12] reported that age hardening occurs via the formation of a metastable $Cu_4Ti$ phase, whereas overaging causes a phase transformation from the metastable and coherent β′-$Cu_4Ti$ phase to the equilibrium and incoherent $Cu_3Ti$ phase and, thus, substantially decreases the strength of Cu–Ti alloy. However, the presence of solute Ti atoms results in an unavoidable decrease in the alloy's electrical conductivity. Extensive efforts have been devoted to enhancing the electrical conductivity of binary Cu–Ti alloys by ternary additions [13–19]. Konno *et al.* [18] reported that the addition of Al causes the formation of the $AlCu_2Ti$ ternary phase and reduces the solute Ti concentration in the Cu matrix, resulting in a decrease of the electrical resistivity. Semboshi and Konno [19] observed that, because of the formation of $TiH_2$, the electrical conductivity of Cu–3at%Ti alloy aged at 773 K in a hydrogen atmosphere was increased by three times compared to that of Cu–3at%Ti alloy aged under vacuum.

Because the addition of Ni to Cu–Ti alloy can form a $Ni_3Ti$ intermetallic compound, its addition decreases the solubility of Ti in the Cu matrix, reduces electron scattering, and improves the electrical conductivity of Cu–Ti alloys.

Corresponding author: Xian-hui Wang E-mail: xhwang693@xaut.edu.cn

Thus, the addition of Ni is expected to result in a Cu–Ti–Ni alloy with a good combination of mechanical strength and electrical conductivity. In the present work, the effects of Ni addition and aging treatments on the microstructure and properties of Cu–Ti alloy were studied. The microstructure and precipitation phases were characterized by X-ray diffraction (XRD), scanning electron microscopy (SEM), and transmission electron microscopy (TEM), and the hardness, electrical conductivity, and elastic modulus were tested as well. The purpose of this work was to clarify the aging behavior of ternary Cu–Ti–Ni alloy by structural characterization and mechanical and electrical measurements.

## 2. Experimental

Button ingots with a nominal composition of Cu–3Ti–*x*Ni ($x$ = 0, 1, 5) were prepared by arc-melting in a non-consumable vacuum furnace using 99.9wt% electrolytic copper, 99.9wt% titanium, and 99.9wt% nickel as starting materials. Each ingot was melted at least four times to guarantee its homogeneity. The ingots were cut into blocks, which were then solution-treated at 850°C for 4 h, followed by water quenching. The blocks were aged at 300°C for 2 h and then aged at 450°C for 1, 3, 5, 7, or 11 h under an argon atmosphere (two-step aging). The specimens for microstructural examination were prepared by being mechanically polished and subsequently etched in a solution of 5 g $FeCl_3$, 15 mL HCl, and 100 mL distilled water. The phase constituents were characterized by an XRD-7000S X-ray diffractometer. The morphology and size of the precipitated phases were characterized using a JSM-6700F field-emission scanning electron microscope and a JEM-2100HR high-resolution transmission electron microscope. The specimens used for TEM observations were cut from the block using a low-speed Isomet cutting machine and then mechanically polished to obtain 50 μm thick slices. Discs of 3 mm in diameter were punched from these slices and thinned in a M691 ion milling machine at 4.5 kV. The electrical conductivity, hardness, and elastic modulus were tested using a FQR-7501 eddy conductivity gauge, an HV-1000 hardness testing machine at a load of 100 N and a holding time of 10 s, and an Agilent G200 Nano Indenter, respectively.

## 3. Results and discussion

### 3.1. Microstructural characterization

3.1.1. X-ray diffraction

Fig. 1 shows the XRD patterns of the as-cast Cu–3Ti–1Ni and Cu–3Ti–5Ni alloys. As seen from Fig. 1, the NiTi phase and Cu phase coexist in the as-cast Cu–3Ti–5Ni alloy, whereas only a single Cu phase presents in the as-cast Cu–3Ti–1Ni alloy because the small amount of NiTi phase present in the Cu–3Ti–1Ni alloy was beyond the limit of detection of the instrument. To better understand the microstructural evolution clearly, the microstructural evolution and phase constituents of the aged Cu–3Ti–5Ni alloy were investigated. Fig. 2 shows the microstructure of the as-cast Cu–3Ti–5Ni alloy. It can be seen from Fig. 2 that the NiTi phase presents in stripes and spherical shape in the Cu matrix.

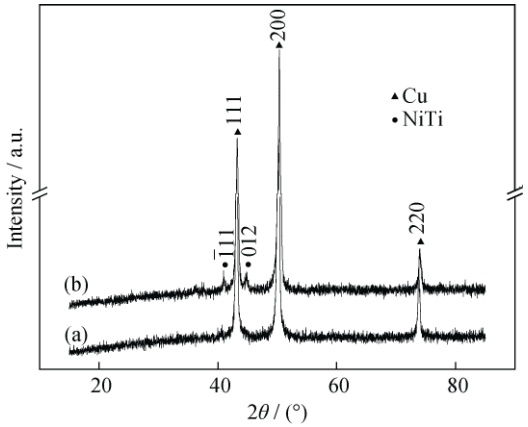


**Fig. 1. XRD patterns of the Cu–3Ti–*x*Ni alloy: (a) $x$ = 1 and (b) $x$ = 5.**

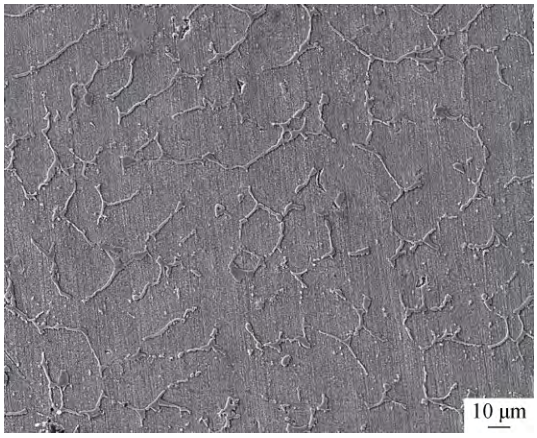


**Fig. 2. As-cast microstructure of the Cu–3Ti–5Ni alloy.**

3.1.2. SEM analysis

Figs. 3(a)–3(f) show SEM micrographs of the Cu–3Ti–5Ni alloy specimens after different aging treatments. As shown in Fig. 3(a), the secondary phase appeared as spot shapes after the alloy was aged at 300°C for 2 h and 450°C for 1 h. In the case of the specimen aged at 300°C for 2 h and 450°C for 3 h, the amount of the spot phase decreased and an acicular phase appeared, as shown in Fig. 3(b). As shown in Fig. 3(c), the amount of the spot phase decrease significantly in

the specimen aged at 300°C for 2 h and 450°C for 5 h. In the case of the specimen aged at 300°C for 2 h and 450°C for 7 h, the spot phase disappeared and the acicular phase was uniformly distributed in the Cu matrix (Fig. 3(d)). However, the primary NiTi phase became irregular particles in the specimen aged at 300°C for 2 h and 450°C for 11 h (Fig. 3(e)) compared with the as-cast microstructure (see Fig. 2). Fig. 3(f) shows a high-magnification image of the micrograph in Fig. 3(e). Irregular particles were clearly distributed in the Cu matrix. With increasing aging time, a portion of the NiTi phase decomposed into Ni and Ti atoms, which dissolved into the Cu matrix, giving rise to a change from the striped and spherical NiTi phase to irregular particles in overaged specimens.

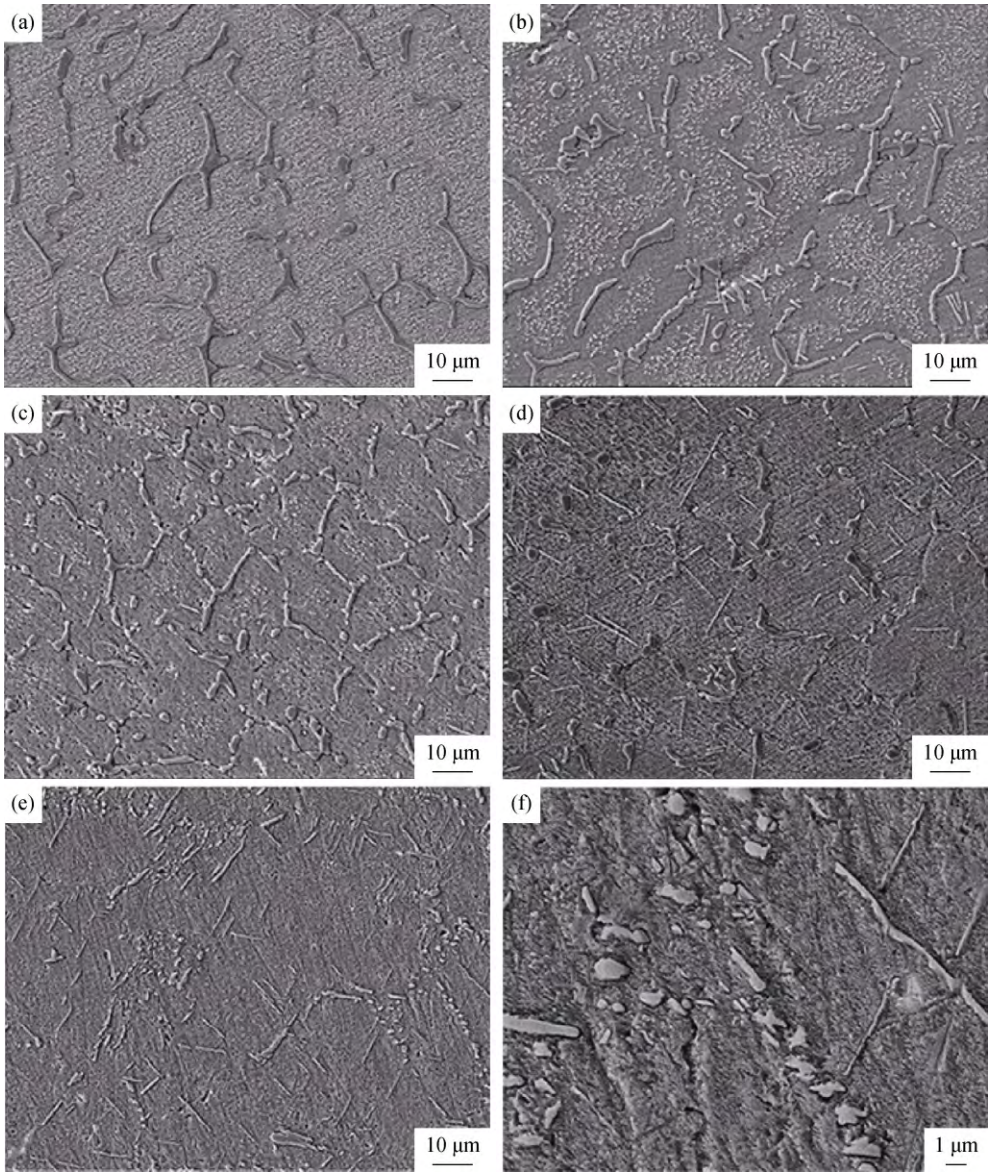


**Fig. 3. SEM micrographs of the Cu–3Ti–5Ni alloy aged at 300°C for 2 h and then aged at 450°C for different time: (a) 1 h, (b) 3 h, (c) 5 h, (d) 7 h, and (e) 11 h; (f) micrograph in Fig. 3(e) at high magnification.**

3.1.3. TEM analysis

To further determine the phase constituents and morphology of aged Cu–3Ti–5Ni alloy, the Cu–3Ti–5Ni alloy aged at 300°C for 2 h and 450°C for 7 h was characterized by XRD and TEM. Fig. 4 presents the XRD pattern of the aged Cu–3Ti–5Ni alloy. Obviously, β′-$Ni_3Ti$ and β′-$Cu_4Ti$ precipitated phases presented after the aging treatment, in addition to a residual NiTi phase. Figs. 5(a), 5(b), and 5(c) are a TEM micrograph of Cu–3Ti–5Ni alloy aged at 300°C for 2 h and 450°C for 7 h, the selected-area diffraction (SAD) pattern with the electron beam parallel to $[1\bar{1}2]_\alpha$, and its schematic, respectively. As evident in Fig. 5(a), the width of

the acicular phase was approximately 100 nm. From Figs. 5(b) and 5(c), it is determined that the acicular phase is β′-$Ni_3Ti$, which has a hexagonal structure with lattice parameters of $a$ = 0.5092 nm, $b$ = 0.5092 nm, and $c$ = 0.8297 nm.

Fig. 6(a) shows another small, precipitated phase with a width of approximately 10 nm distributed in the Cu matrix. Figs. 6(b) and 6(c) show the SAD pattern obtained with the electron beam parallel to $[004]_\alpha$ and its schematic, respectively. As evident in Figs. 6(b) and 6(c), the tiny precipitated phase is β′-$Cu_4Ti$. Analysis of the SAD pattern indicated that $Cu_4Ti$ has an orthorhombic structure with lattice parameters of $a$ = 0.453 nm, $b$ = 0.4342 nm, and $c$ = 1.293 nm.

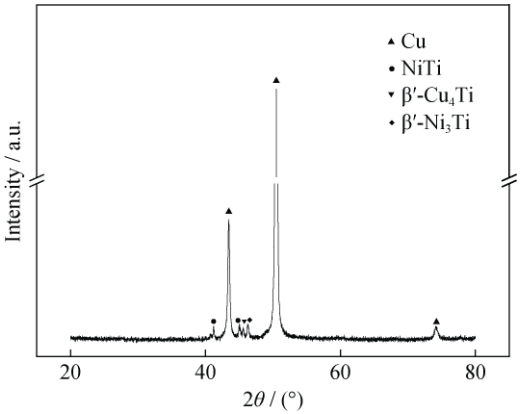


**Fig. 4. XRD pattern of the Cu–3Ti–5Ni alloy aged at 300°C for 2 h and 450°C for 7 h.**

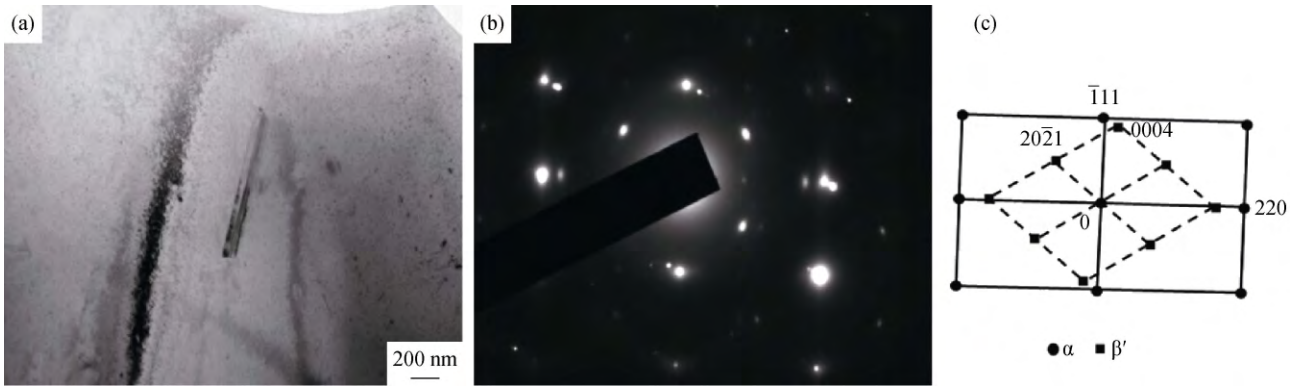


**Fig. 5. TEM images of the Cu–3Ti–5Ni alloy aged at 300°C for 2 h and 450°C for 7 h: (a) micrograph, (b) SAD pattern, and (c) schematic of the SAD pattern.**

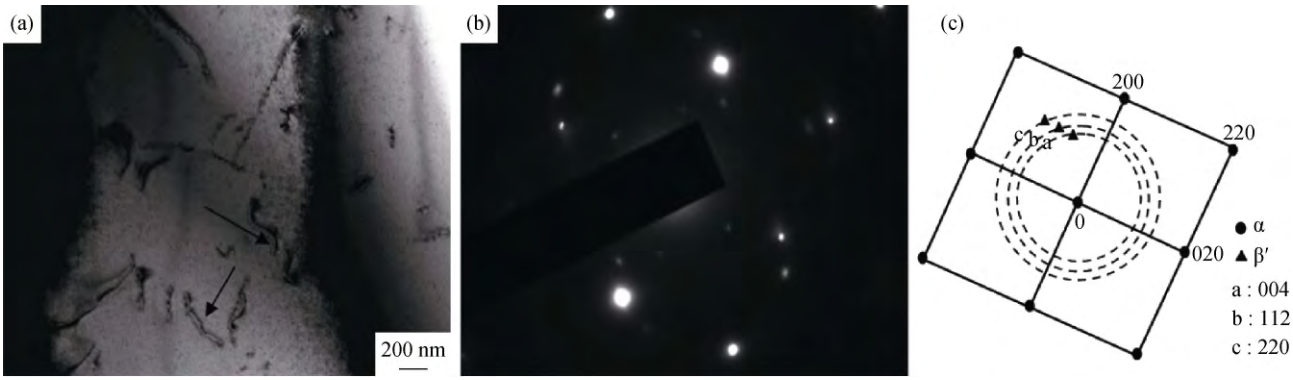


**Fig. 6. TEM images of the Cu–3Ti–5Ni alloy aged at 300°C for 2 h and 450°C for 7 h: (a) micrograph, (b) SAD pattern, and (c) schematic of the SAD pattern.**

The spherical phase in the Cu–3Ti–5Ni alloy aged at 300°C for 2 h and 450°C for 7 h was also analyzed by TEM. Fig. 7(a) shows that the size of the spherical phase was approximately 1.6 μm. As evident from the SAD pattern obtained with the electron beam parallel to $[003]_\beta$ and its schematic, this phase is the residual NiTi phase (see Figs. 7(b) and 7(c)). Analysis of the SAD pattern indicated that the NiTi phase has a monoclinic structure with lattice parameters of $a$ = 0.2885 nm, $b$ = 0.4622 nm, and $c$ = 0.412 nm. Notably, annealing twins present in the NiTi phase.

### 3.2. Physical and electrical properties of Cu–Ti–Ni alloy

3.2.1. Hardness

The variation of hardness with secondary aging time for the Cu–3Ti–$x$Ni ($x$ = 0, 1, 5) alloys is shown in Fig. 8. The hardness increased and then decreased with increasing secondary aging time. After being aged at 300°C for 2 h and 450°C for 7 h, the Cu–3Ti, Cu–3Ti–1Ni, and Cu–3Ti–5Ni

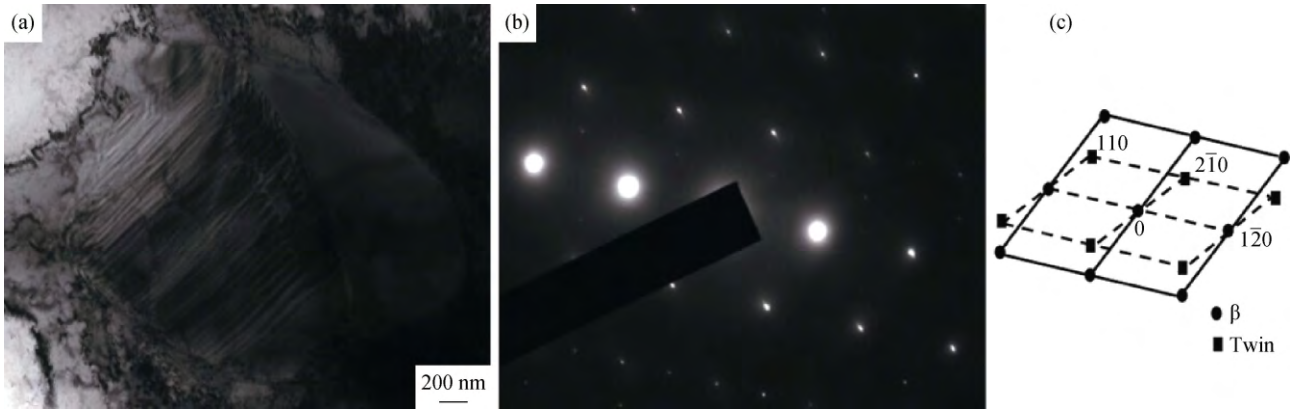


**Fig. 7. TEM images of the Cu–Ti–5Ni alloy aged at 300°C for 2 h and 450°C for 7 h: (a) micrograph, (b) SAD pattern, and (c) schematic of the SAD pattern.**

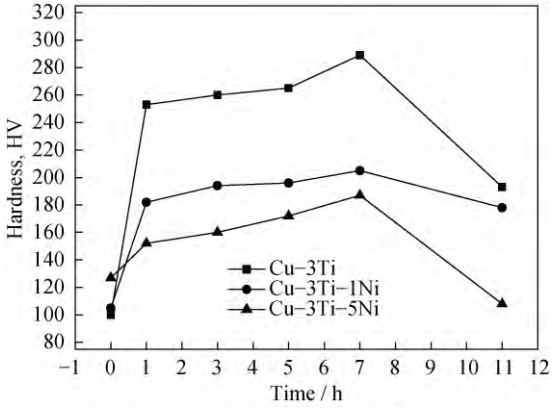


**Fig. 8. Variation of the hardness with secondary aging time for the Cu–3Ti–*x*Ni (*x* = 0, 1, 5) alloys.**

alloys reach their peak hardness of HV 289, HV 205, and HV 187, respectively. As previously mentioned, the β′-$Ni_3Ti$ and β′-$Cu_4Ti$ phases that continuously precipitate from the supersaturated Cu matrix during the aging process result in increased hardness. However, excessive aging gives rise to partial dissolution of the NiTi phase into the Cu matrix and the phase transformation from the metastable and coherent β′-$Cu_4Ti$ phase to the equilibrium and incoherent $Cu_3Ti$ phase [15–17], resulting in decreased hardness. The addition of excessive Ni was also observed to decrease the hardness of Cu–3Ti alloy.

3.2.2. Electrical conductivity

Fig. 9 shows the variation of electrical conductivity with secondary aging time for the Cu–3Ti–*x*Ni (*x* = 0, 1, 5) alloys. The electrical conductivity of the three alloys increased sharply after they were aged at 300°C for 2 h and 450°C for 1 h and then increased slightly with increasing secondary aging time. After aging at 300°C for 2 h and 450°C for 7 h, the Cu–3Ti, Cu–3Ti–1Ni, and Cu–3Ti–5Ni alloys exhibited electrical conductivities of 15.79% IACS, 18.2% IACS, and 31.32% IACS, respectively. However, the electrical conductivity decreased when the aging time was excessive. After aging at 300°C for 2 h and 450°C for 11 h, the electrical conductivities of the Cu–3Ti–1Ni and Cu–3Ti–5Ni alloys were 17.2% IACS and 22.97% IACS, respectively.

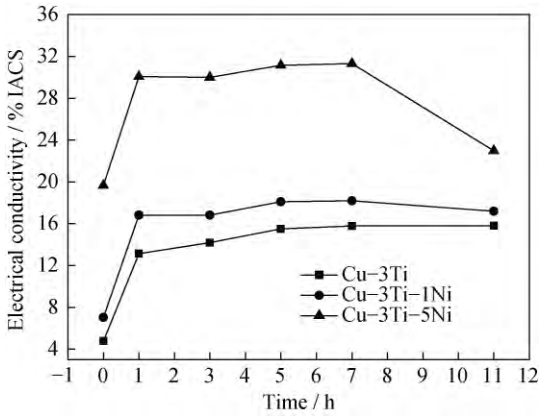


**Fig. 9. Variation of the electrical conductivity with secondary aging time for the Cu–3Ti–*x*Ni (*x* = 0, 1, 5) alloys.**

The solubility of alloying elements in the Cu matrix is a dominant factor governing the electrical conductivity of the alloys. The increased electrical conductivity is attributed to the precipitation of β′-$Ni_3Ti$ and β′-$Cu_4Ti$ from the Cu matrix, which decreases lattice distortion and electron scattering. Nevertheless, excessive aging promotes partial dissolution of alloying elements into the Cu matrix, which increases the lattice distortion and the electron scattering, thus resulting in a decrease of the electrical conductivity.

3.2.3. Elastic modulus

Table 1 lists the elastic modulus of as-cast Cu–3Ti–*x*Ni (*x* = 0, 1, 5) and Cu–3Ti–*x*Ni (*x* = 0, 1, 5) alloys aged at 300°C for 2 h and 450°C for 7 h. Compared with the as-cast Cu–3Ti–*x*Ni (*x* = 0, 1, 5) alloys, the elastic modulus increased slightly after aging. The possible reason for this increase is that the precipitation of β′-$Ni_3Ti$ and β′-$Cu_4Ti$ phases enhanced the strength of the Cu–3Ti–*x*Ni (*x* = 0, 1, 5)

alloys, giving rise to a slight increase in the elastic modulus. However, this finding is not consistent with the conventional viewpoint that, in general, the elastic modulus of metallic materials is insensitive to microstructure [20–21]. More research is necessary to understand this phenomenon.

**Table 1. Elastic modulus of the as-cast and aged Cu–3Ti–*x*Ni (*x* = 0, 1, 5) alloys** GPa

| Alloy | Cu–3Ti | Cu–3Ti–1Ni | Cu–3Ti–5Ni |
|---|---|---|---|
| As-cast | 127 | 138 | 140 |
| Aged at 300°C for 2 h and 450°C for 7 h | 135 | 146 | 147 |

## 4. Conclusions

(1) The microstructure of the as-cast Cu–3Ti–1Ni alloy and Cu–3Ti–5Ni alloy consisted of NiTi phase and Cu phase.

(2) β′-$Ni_3Ti$ and β′-$Cu_4Ti$ phases precipitated from the Cu matrix after an appropriate aging treatment, and the formation of NiTi, β′-$Ni_3Ti$, and β′-$Cu_4Ti$ resulted in increased electrical conductivity.

(3) Ni addition enhanced the electrical conductivity but decreased the hardness of Cu–3Ti alloy.

(4) After a two-step aging treatment at 300°C for 2 h and 450°C for 7 h, the Cu–3Ti–5Ni alloy exhibited good combined properties. The hardness, electrical conductivity, and elastic modulus of the Cu–3Ti–5Ni alloy were HV 187, 31.32% IACS, and 147 GPa, respectively.

## Acknowledgements

This research was financially supported by the National Natural Science Foundation of China (Nos. 51201132 and 51274163), the Research Program of Shaanxi Provincial Key Laboratory (No. 13JS076), the China Scholarship Council, the Pivot Innovation Team of Shaanxi Electrical Materials and Infiltration Technique (No. 2012KCT-25), and the Shaanxi Provincial Project of Special Foundation of Key Disciplines (No. 2011HBSZS009).

## References

[1] G.L. Xie, Q.S. Wang, X.J. Mi, B.Q. Xiong, and L.J. Peng, The precipitation behavior and strengthening of a Cu–2.0wt% Be alloy, *Mater. Sci. Eng. A.*, 558(2012), p. 326.

[2] W.A. Soffa and D.E. Laughlin, High-strength age hardening copper-titanium alloys: redivivus, *Prog. Mater. Sci.*, 49(2004), No. 3-4, p. 347.

[3] R. Markandeya, S. Nagarjuna, D.V.V. Satyanarayana, and D.S. Sarma, Correlation of structure and flow behavior of Cu–Ti–Cd alloys, *Mater. Sci. Eng. A*, 428(2006), No. 1-2, p. 233.

[4] V. Lebreton, D. Pachoutinski, and Y. Bienvenu, An investigation of microstructure and mechanical properties in Cu-Ti-Sn alloys rich in copper, *Mater. Sci. Eng. A*, 508(2009), No. 1-2, p. 83.

[5] M. Sobhani, A. Mirhabibi, H. Arbi, and R.M.D. Brydson, Effects of in situ formation of $TiB_2$ particles on age hardening behavior of Cu–1wt% Ti–1wt% $TiB_2$, *Mater. Sci. Eng. A*, 577(2013), p. 16.

[6] R. Markandeya, S. Nagarjuna, and D.S. Sarma, Characterization of prior cold worked and age hardened Cu–3Ti–1Cd alloy, *Mater. Charact.*, 54(2005), No. 4-5, p. 360.

[7] S. Nagarjuna, M. Srinivas, K. Balasubramanian, and D.S. Sarma, On the variation of mechanical properties with solute content in Cu–Ti alloys, *Mater. Sci. Eng. A*, 259(1999), No. 1, p. 34.

[8] D. Božić, O. Dimčić, B. Dimčić, I. Cvijović, and V. Rajković, The combination of precipitation and dispersion hardening in powder metallurgy produced Cu–Ti–Si alloy, *Mater. Charact.*, 59(2008), No. 8, p. 1122.

[9] R. Markandeya, S. Nagarjuna, and D.S. Sarma, Effect of prior cold work on age hardening of Cu–4Ti–1Cr alloy, *Mater. Sci. Eng. A*, 404(2005), No. 1-2, p. 305.

[10] S. Nagarjuna, U.C. Babu, and P. Ghosal, Effect of cryo-rolling on age hardening of Cu–1.5Ti alloy, *Mater. Sci. Eng. A*, 491(2008), No. 1-2, p. 331.

[11] S. Nagarjuna, K. Balasubramanian, and D.S. Sarma, Effects of cold work on precipitation hardening of Cu–4.5 mass% Ti alloy, *Mater. Trans. JIM*, 36(1995), No. 8, p. 1058.

[12] R. Markandeya, S. Nagarjuna, and D.S. Sarma, Influence of prior cold work on age hardening of Cu–Ti–Zr alloys, *Mater. Sci. Technol.*, 21(2005), No. 10, p. 1171.

[13] S. Nagarjuna, K. Balasubramanian, and D.S. Sarma, Effect of Ti additions on the electrical resistivity of copper, *Mater. Sci. Eng. A*, 225(1997), No. 1-2, p. 118.

[14] R. Markandeya, S. Nagarjuna, and D.S. Sarma, Precipitation hardening of Cu–Ti–Cr alloys, *Mater. Sci. Eng. A*, 371(2004), No. 1-2, p. 291.

[15] R. Markandeya, S. Nagarjuna, and D.S. Sarma, Precipitation hardening of Cu–3Ti–1Cd alloy, *J. Mater. Eng. Perform.*, 16(2007), No. 5, p. 640.

[16] R. Markandeya, S. Nagarjuna, and D.S. Sarma, Precipitation hardening of Cu–4Ti–1Cd alloy, *J. Mater. Sci.*, 39(2004), No. 5, p. 1579.

[17] R. Markandeya, S. Nagarjuna, and D.S. Sarma, Effect of prior cold work on age hardening of Cu–3Ti–1Cr alloy, *Mater. Charact.*, 57(2006), No. 4-5, p. 348.

[18] T.J. Konno, R. Nishio, S. Semboshi, T. Ohsuna, and E. Okunishi, Aging behavior of Cu–Ti–Al alloy observed by transmission electron microscopy, *J. Mater. Sci.*, 43(2008), No. 11, p. 3761.

[19] S. Semboshi and T.J. Konno, Effect of aging in hydrogen atmosphere on electrical conductivity of Cu–3at.%Ti alloy, *J. Mater. Res.*, 23(2008), No. 2, p. 473.

[20] M. Kikuchi, M. Takahashi, and O. Okuno, Elastic moduli of cast Ti–Au, Ti–Ag, and Tι–Cu alloys, *Dent. Mater.*, 22(2006), No. 7, p. 641.

[21] K. Fujiwara, H. Tanimoto, and H. Mizubayashi, Elasticity study of very thin Cu films, *Mater. Sci. Eng. A*, 442(2006), No. 1-2, p. 336.